**Supplemental Document 1**

**for**

**“Selection of robust metrics for the position and width of hyperspectral response functions via a simulation approach”**

(Please note *main document sections and figure numbers* near the top of following pages that help the reader associate each supplemental page with a particular manuscript section or figure)

### 3.2 Lab collection parameter variations (Supplemental information on hyperspectral camera characterization)

A complete hyperspectral camera characterization includes laboratory and other evaluations that document all aspects of its behavior, including top-level operating features, spectral and spatial response details, radiometric and temporal properties, calibration factors, electro-optical interfacing, and environmental effects and limitations.

This paper is mainly concerned with metrics that document the width and center of the camera's spatial and spectral responses (i.e., those of its two orthogonal LSF's and its SRF). Determination of these quantities thus comprises one part of a full camera characterization.

A variety of electro-optical test configurations are capable of producing the lab data required to compute these metrics. One such approach is shown in block diagram form in Fig. S1.

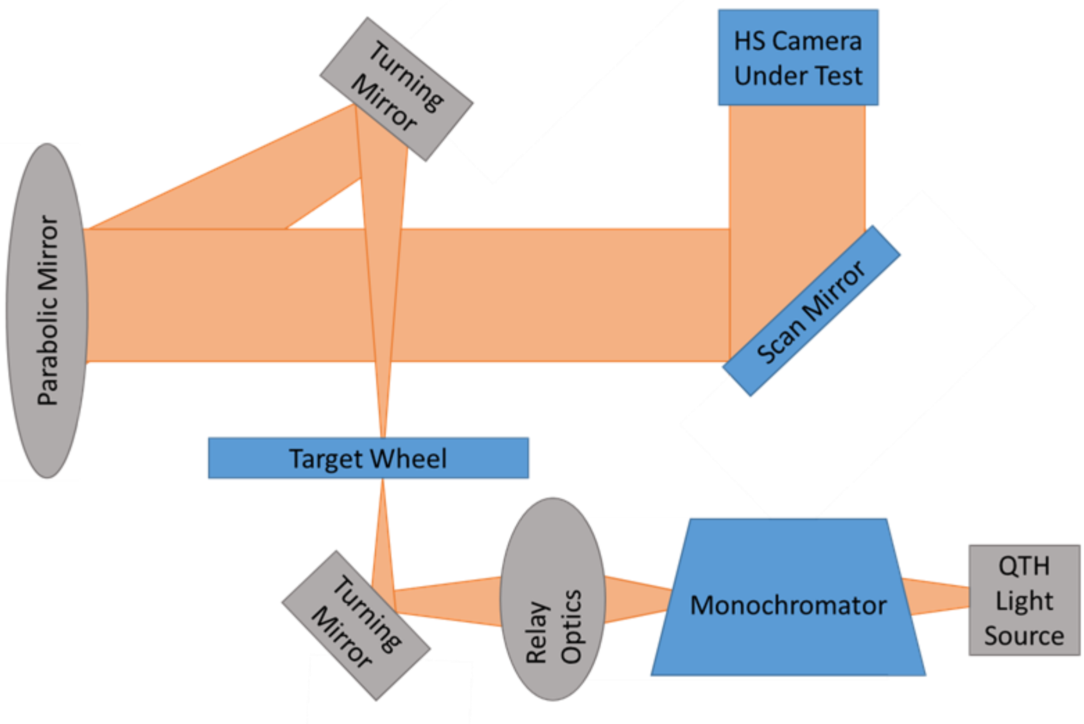


**Figure S1.** Block diagram for a particular SRF / LSF test setup. The target wheel contains selectable slit targets of various widths needed to accommodate a variety of anticipated sensor IFOV's and test types. A two-axis scan mirror facilitates precise positioning of the projected test image relative to an assumed line-scan camera slit. The monochromator is used in first-order mode for SRF work, while LSF testing is performed via its zero-order "white light" mode (or by simply replacing the components preceding the first turning mirror with a broadband source). Orthogonal LSF scans are obtained by rotating the HS camera by 90 degrees about its optical axis.

This setup is capable of projecting both broadband and near-monochromatic slit images whose spatial extent is determined by the EFL of the parabolic mirror and the width of the slit target selected by the target wheel. A computer control system such as that depicted in Fig. S2 is used to systematically step either the apparent position or wavelength of the test image, depending upon the type of test being performed.

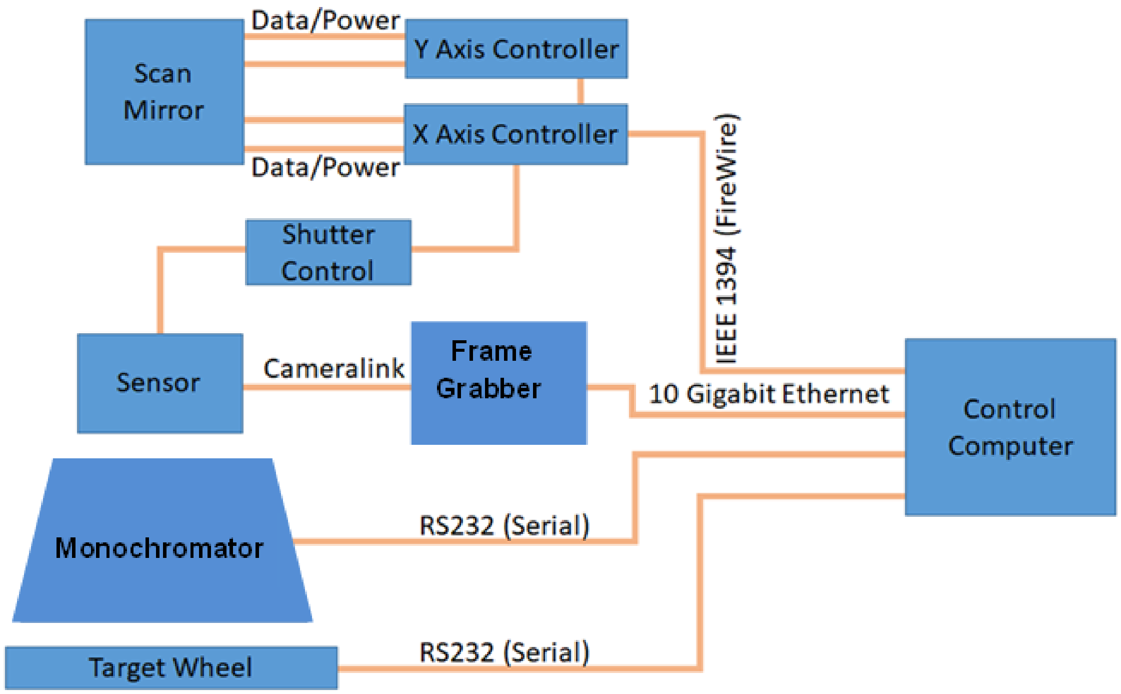


**Figure S2.** Computer interface for SRF/LSF test setup. The control PC is responsible for setting the correct test target (via the target wheel), establishing coarse image positioning within the camera's FOV and wavelength range, performing the fine-scale scan motion sequences (or wavelength changes) needed to sample the LSF or SRF, setting the camera frame rate, integration time, and other parameters, and collecting individual hypercubes at each scan position.

When the position/wavelength sampling and SNR are adequate, plotted camera outputs from these test position sequences closely resemble the overall shape of the LSF or SRF under test, and thus support computation of the metrics under investigation.

Frame averaging may be needed to establish adequate SNR, and significant preliminary work may be needed to establish the interface between a new HS camera type and the control PC, along with possible modifications to the optical system and target wheel targets in order to guarantee that projected test images are of adequately narrow spatial and spectral width.

## 3.2 Lab collection parameter variations (Supplemental information on program implementation)

A given simulation trial is defined by the following user control parameters: (a) camera response function type (i.e., either Normal Distribution or Bi-Normal), (b) the number of random Bi-Normal shapes desired, if this mode has been specified, (c) the response width (i.e., either narrow, typical, or wide), (d) the number of random noise realizations for each tested SNR, and (e) a list of individual center or width algorithms to evaluate.

These inputs are summarized in Table S1, along with key program constants that are discussed in following paragraphs. In both Table S1 and Fig. F2 below, abbreviations ND and BN refer to Normal Distribution and Bi-Normal function shapes respectively. Sample rate is abbreviated as SR.

**Table S1. Summary of User Inputs and Program Constants**

| User Input | Description | Value Range |
|---|---|---|
| Response Type | Specifies camera response function type | ND or BN |
| # of Shapes | Number of random shapes in BN runs | 500 (Typ.) |
| Response Width | Specifies response width category | 0.75, 1.50, or 2.25 Channels |
| # of Trials | Number of noise realizations per SNR | 1000 (ND) or 100 (BN) (Typ.) |
| Algorithm List | One or more center or width alg. names | See main document Section 2 |
| | | |
| **Program Cons.** | **Description** | **Value Range** |
| Resolution | Initial discrete point spacing | 0.005 channels per point |
| Trunc. Limit | Discrete point sequence truncation limit | 1/1024 of response peak |
| SNR | Discrete list of (22) camera SNRs | 10-400 in logarithmic steps |
| SR | Discrete list of (18) test system SRs | 1-20 samples/chan. in log. steps |
| Short Seq. Limit | Rejection criteria for short sequences | Sequence must be > 4 points |
| Error Toler. | Error tolerance on width/center results | ≤ 5%, see text |
| Error Statistic | Error statistic taken across noise trials | Use 95$^{th}$ percentile error |

Computations are carried out within five nested "FOR" loops as depicted in the flow chart of Fig. S3. The first or outermost loop controls the number of response functions under evaluation. It executes one time only for the Normal Distribution shape, or otherwise 500 or more times when simulating an ensemble of randomly-generated Bi-Normal responses.

The second loop (a) specifies the current center or width algorithm under evaluation, and (b) computes a high-resolution (200 points per camera channel) discrete version of the specified Normal Distribution or a new random Bi-Normal shape. This is referred to as the reference sequence in later paragraphs. Response function synthesis equations and parameter ranges are discussed in the main document.

This loop is executed once for each algorithm and shape combination. For example, if six (6) center algorithms are under investigation in the Bi-Normal mode, then typically (6 x 500) or 3000 iterations of the loop are performed. Each algorithm is thereby evaluated via its own unique ensemble of response shapes and associated truth values.

The tails of the reference sequence are truncated at abscissa values where the ordinate first falls below 1/1024 times the peak function value. This arbitrary limit corresponds to 1 bit on a 10-bit digitized signal, or roughly 0.1% of the peak response if test source power and the camera gain have been adjusted appropriately. A "truth" result is computed for the center or width of the reference sequence and saved for later use.

The innermost three loops vary (a) peak imager SNR, (b) the sample rate of the system in samples per camera channel, (c) the phase (or offset) between the data sequence and an arbitrary reference position in the imager's FOV or wavelength range, and (d) the particular noise realization that is added to the reference response. Normally-distributed additive noise is employed in (d) since it closely approximates the Poisson noise that is expected to dominate lab measurements.

In effect, center or width results are computed for all possible SNR and sample rate combinations specified by two individual lists of fixed values. A total of 22 SNRs between 10.5 and 400, and 18 sample rates in the range 1.05 to 20 samples/channel are employed. Individual SNRs and sample rates are varied logarithmically. A given response shape is thus evaluated over (22 x 18) or 396 possible parameter combinations.

Test system sample rate variations are simulated by applying simple downsampling (i.e., without low pass filtering) to the reference response. This is done at each of 18 unique downsample factors determined by the sample rate list and the reference sequence point spacing.

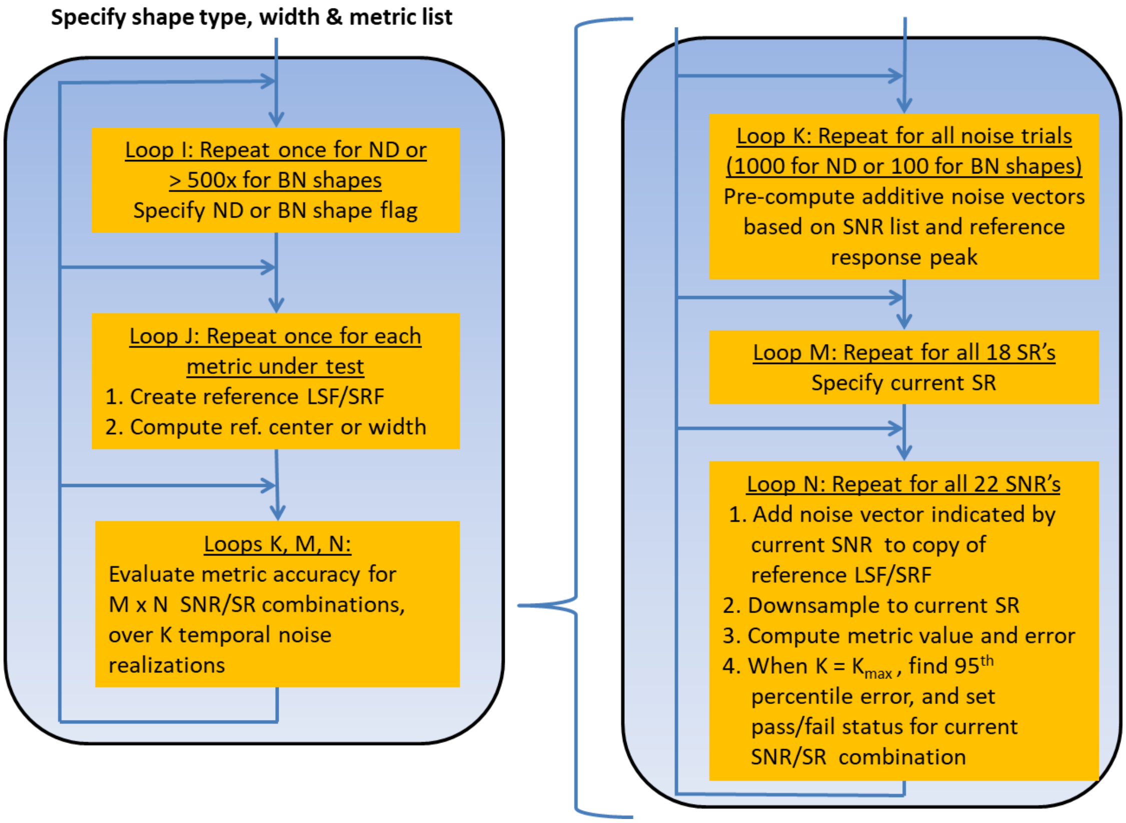


**Figure S3.** Simplified processing flow chart with typical user and program constants from Table S1.

Metric error for a single noise instantiation is computed as the difference between the current metric value (i.e., the result obtained at the bottom of loop N in Fig. S3) and the truth value obtained from the reference response.

Algorithm results for each SNR/sample rate combination are determined over $K_{max}$ random noise realizations. The number of noise realizations is empirically chosen to limit execution time to that required to produce smooth trends in plotted results, while taking into account that the Bi-Normal plots shown in the results section additionally aggregate results over the full ensemble of random response shapes.

Final results for Normal Distribution simulations were obtained by specifying a relatively large number of random noise instantiations ($K_{max}$ = 1000), while Bi-Normal simulations assessed performance over a smaller number of trials ($K_{max}$ =100).

Pass-fail status at a particular SNR/sample rate combination is determined by comparing the 95$^{th}$ percentile error over all noise instantiations to a fixed threshold. Short point sequences that may occur at low sample rates are unconditionally rejected and result in failing status for the current algorithm and SNR/sample rate under test.

An arbitrary center-metric error tolerance of 1/20$^{th}$ or 5% of one spatial channel width was chosen for this work, noting that this is somewhat smaller than typical spectral and spatial coregistration tolerances specified for high quality cameras.

Similarly, a width-metric error tolerance equal to 5% of the reference width was employed, noting for example that this level of width uncertainty on the SRF is thought to be adequate for demanding applications such as model-based atmospheric compensation.

At the end of the simulation process, algorithm results and metadata are saved for later analysis that is accomplished via a separate software program.

This page intentionally left blank.

4.1 Algorithm flexibility (Supplemental information to Fig. 4, center metric results for all response function widths)

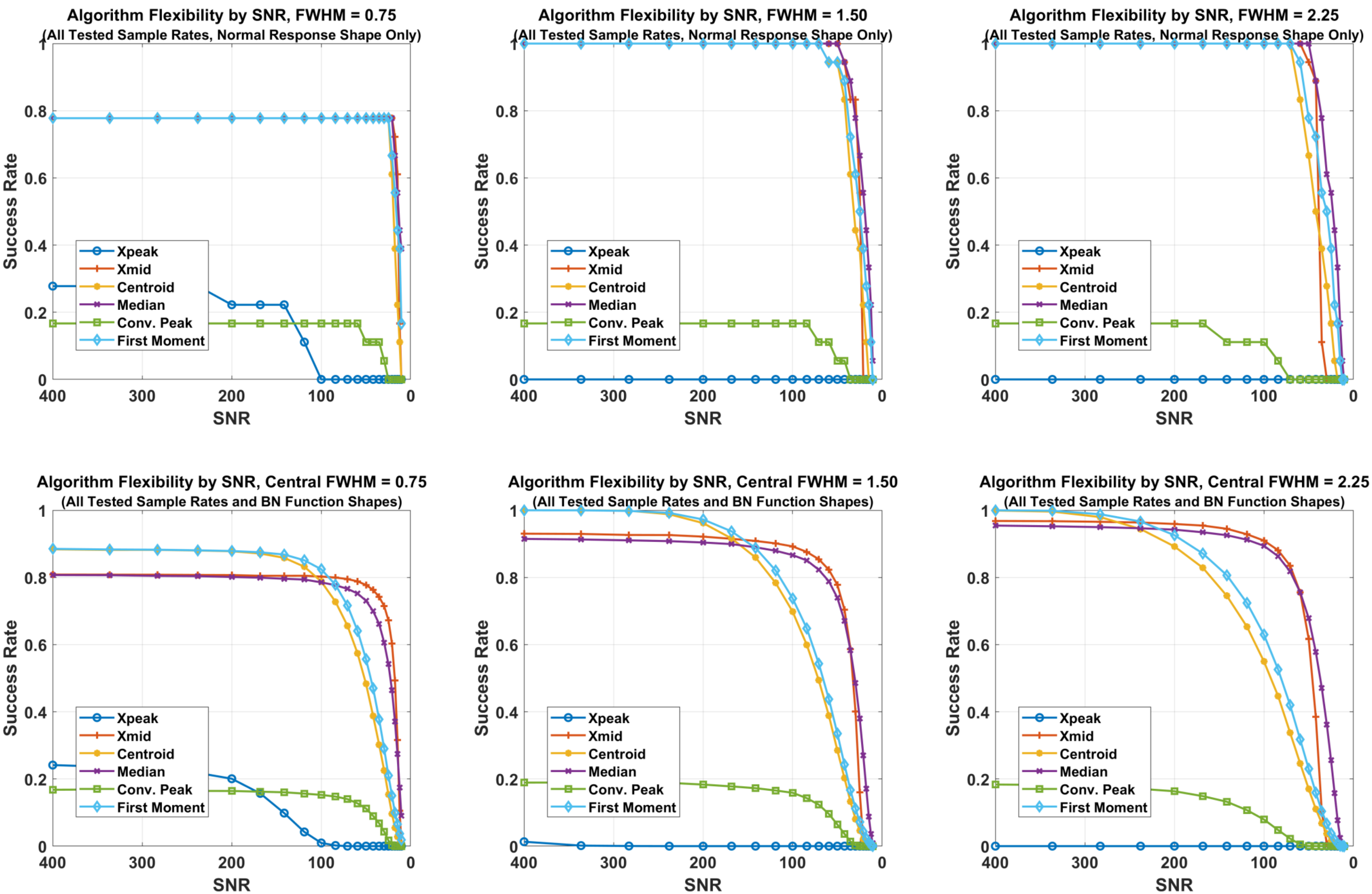

4.1 Algorithm flexibility (Supplemental information to Fig. 5, width metric results for all response function widths)

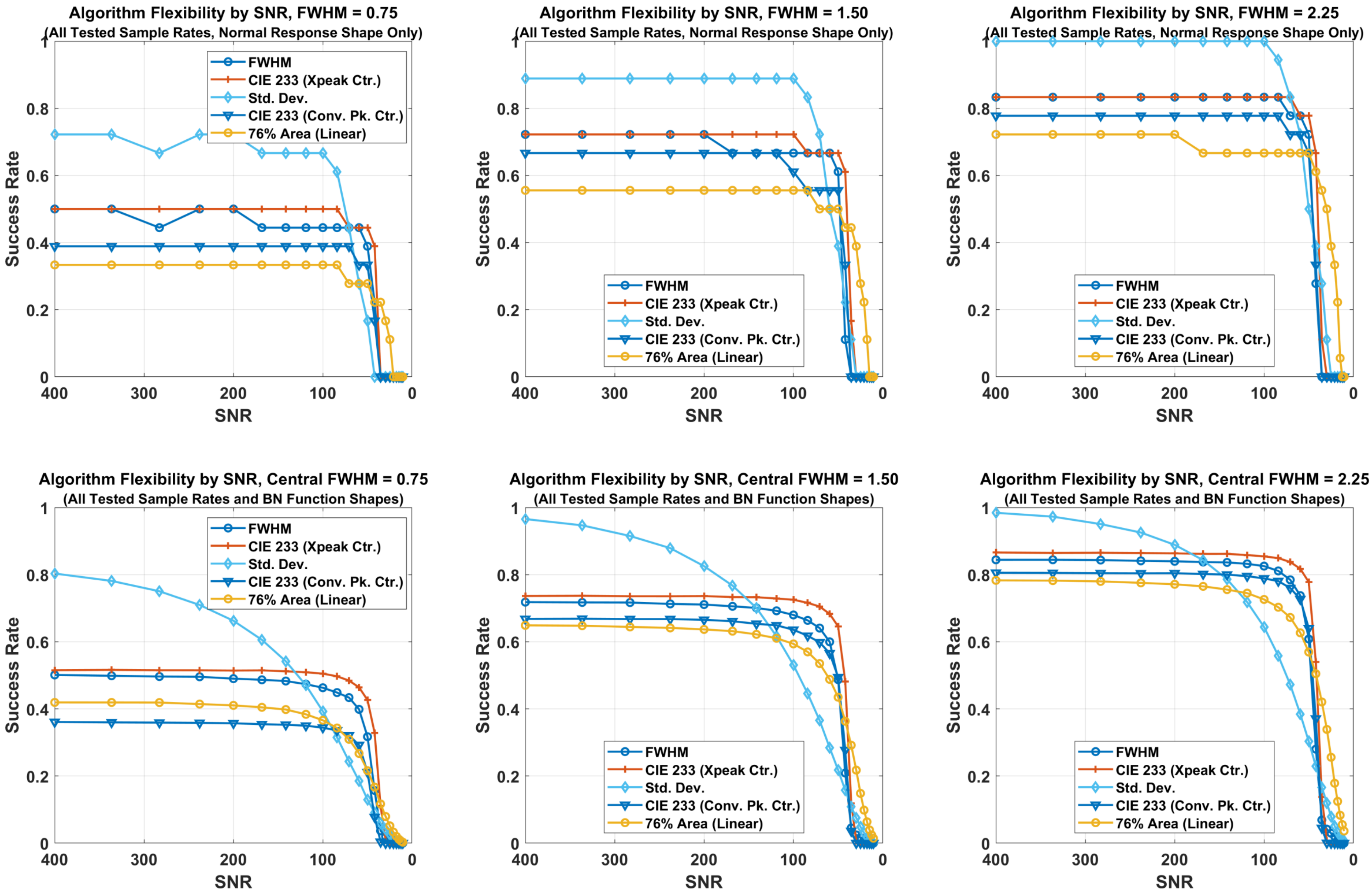

This page intentionally left blank.

4.2 Sample rate trends versus SNR (Supplemental information to Fig. 6, center metric results for all response function widths)

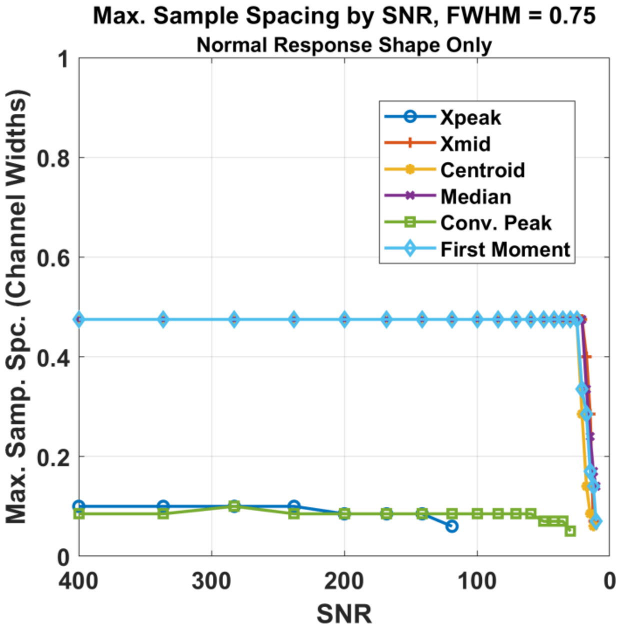


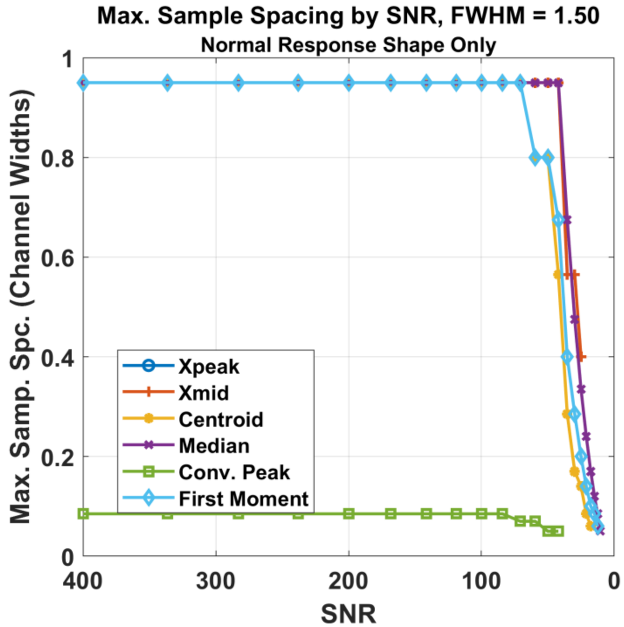


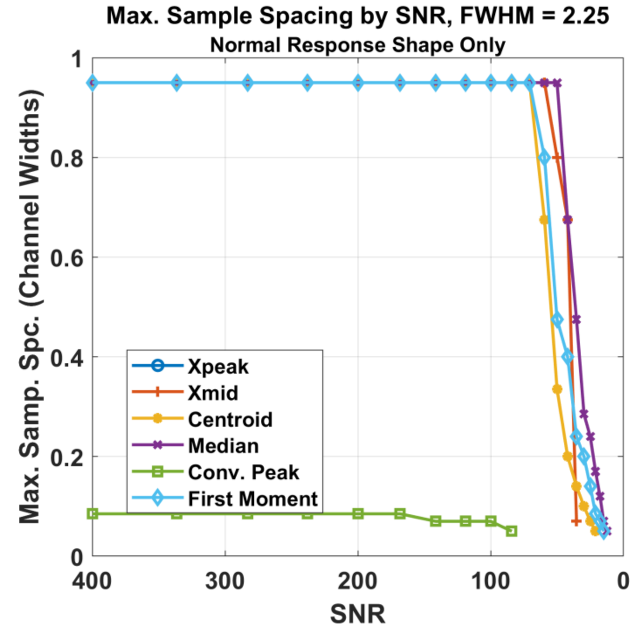


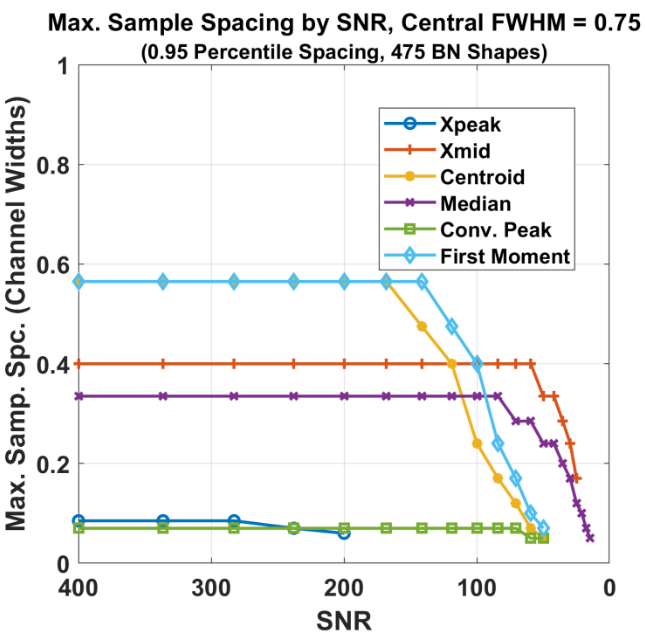


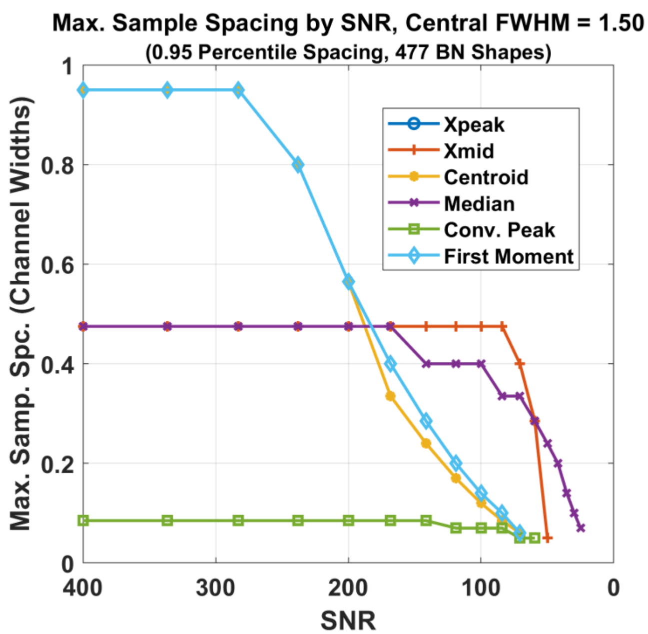


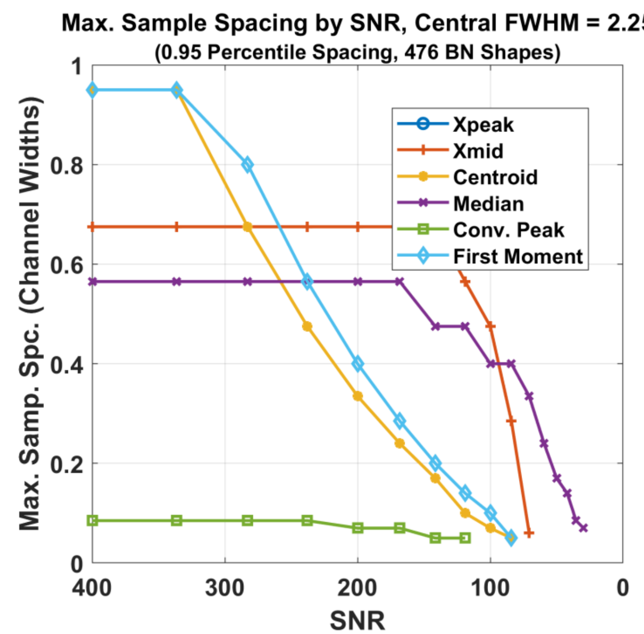

4.2 Sample rate trends versus SNR (Supplemental information to Fig. 7, width metric results for all response function widths)

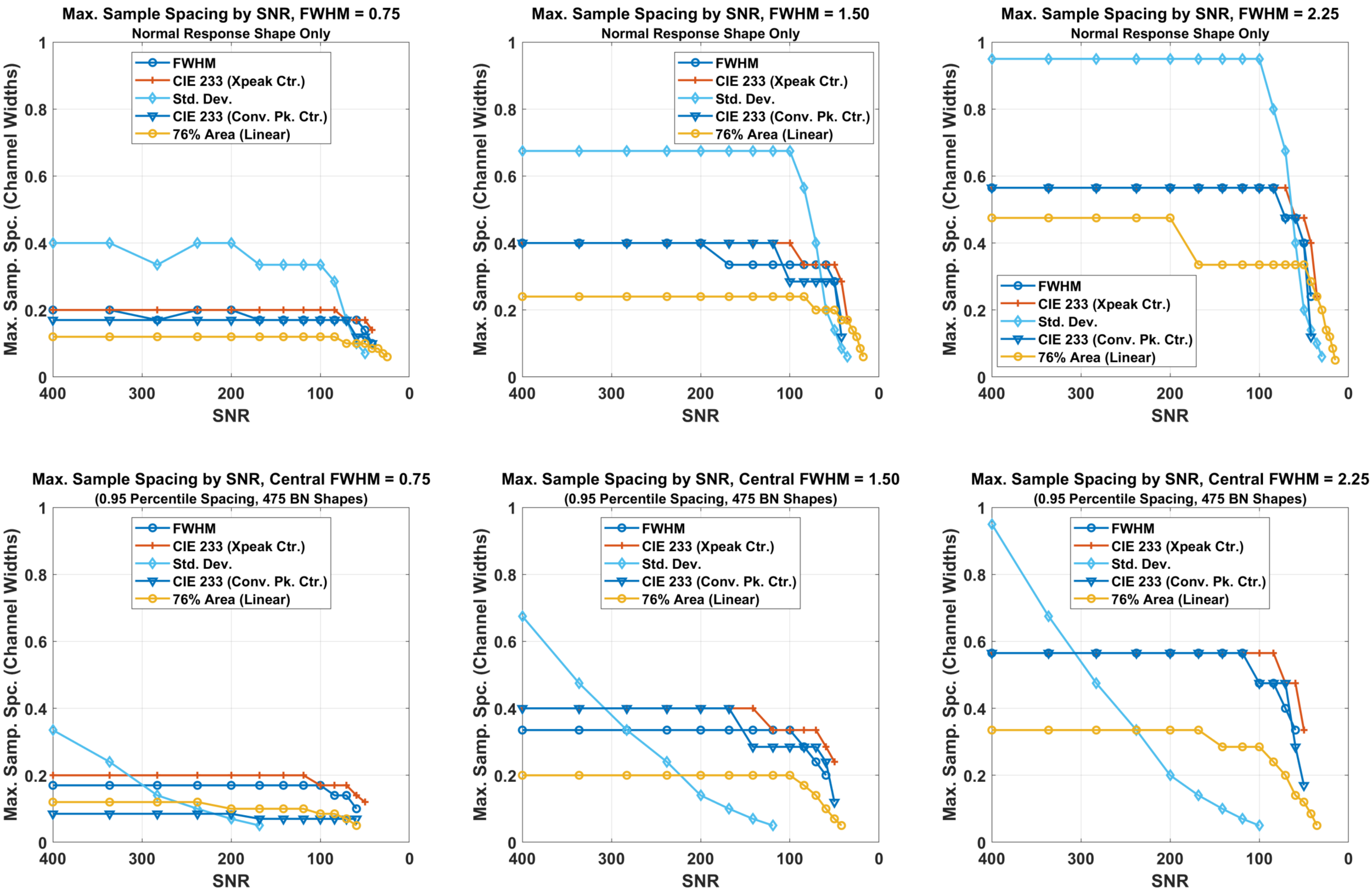

This page intentionally left blank.

4.3 SNR effects on total test time and algorithm selection (Supplemental information to Fig. 8, center metrics, Normal responses, all response widths and K-values)

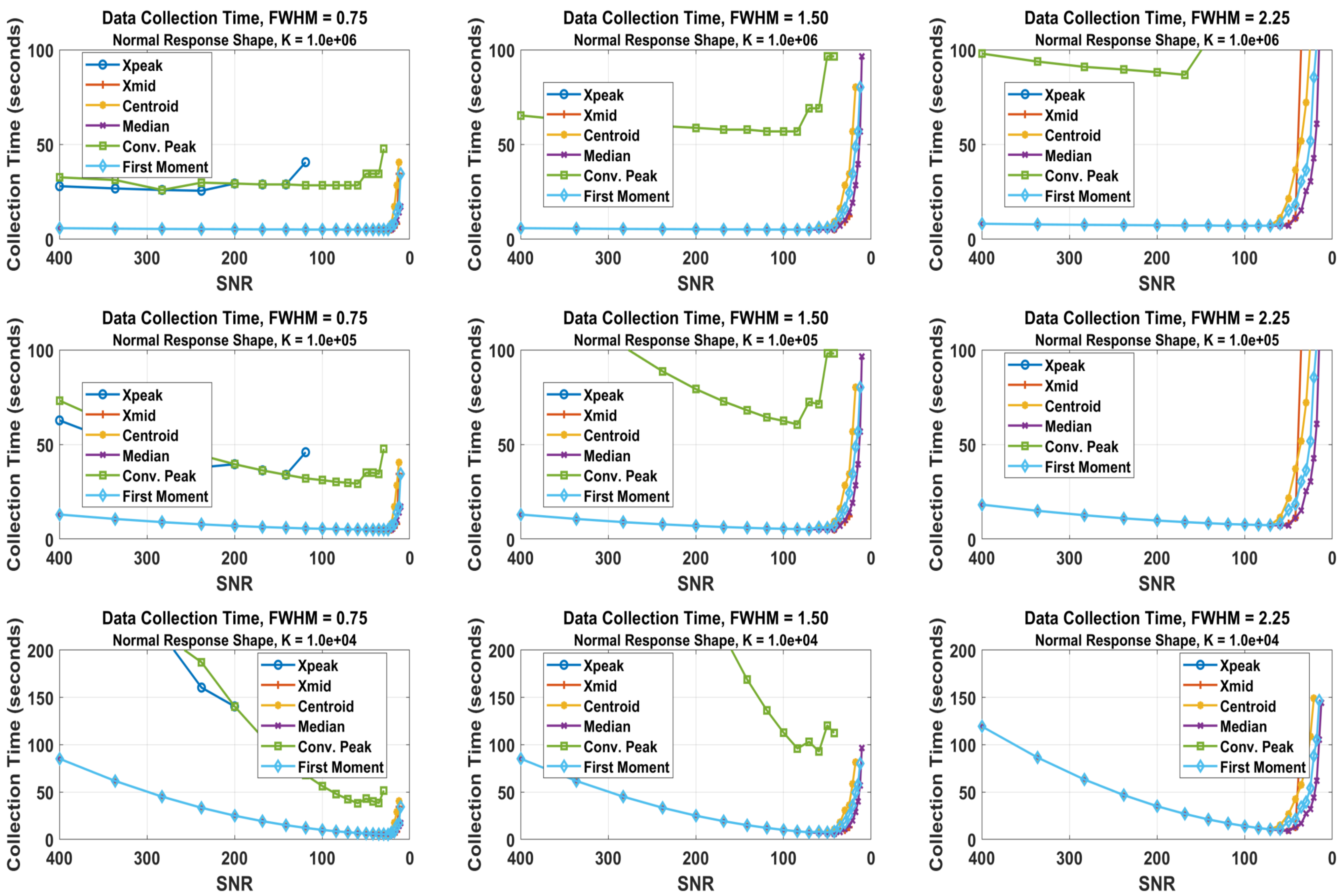

4.3 SNR effects on total test time and algorithm selection (Supplemental information to Fig. 8, center metrics, Bi-Normal responses, all response widths and K-values)

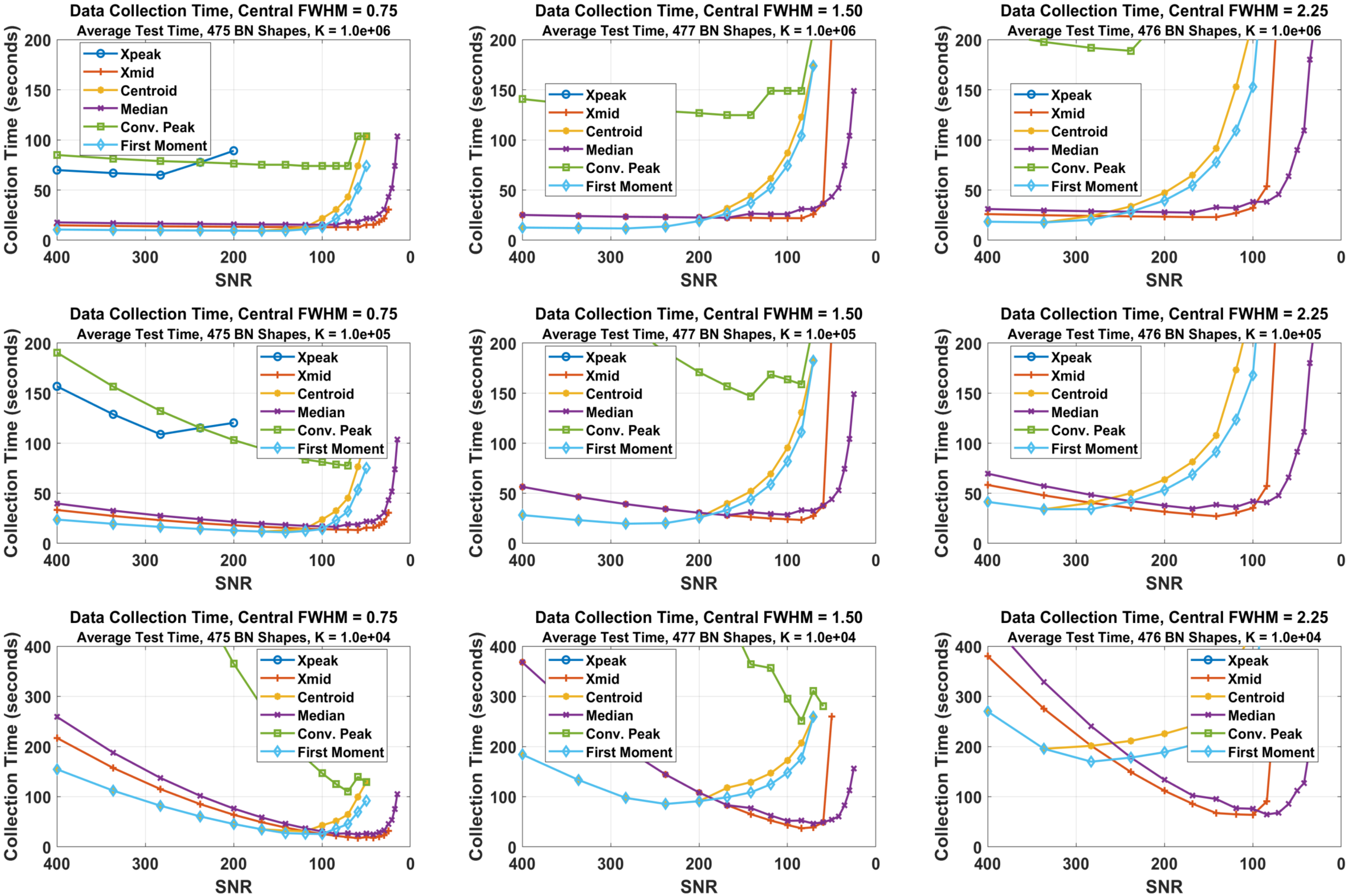

4.3 SNR effects on total test time and algorithm selection (Supplemental information to Fig. 9, width metrics, Normal responses, all response widths and K-values)

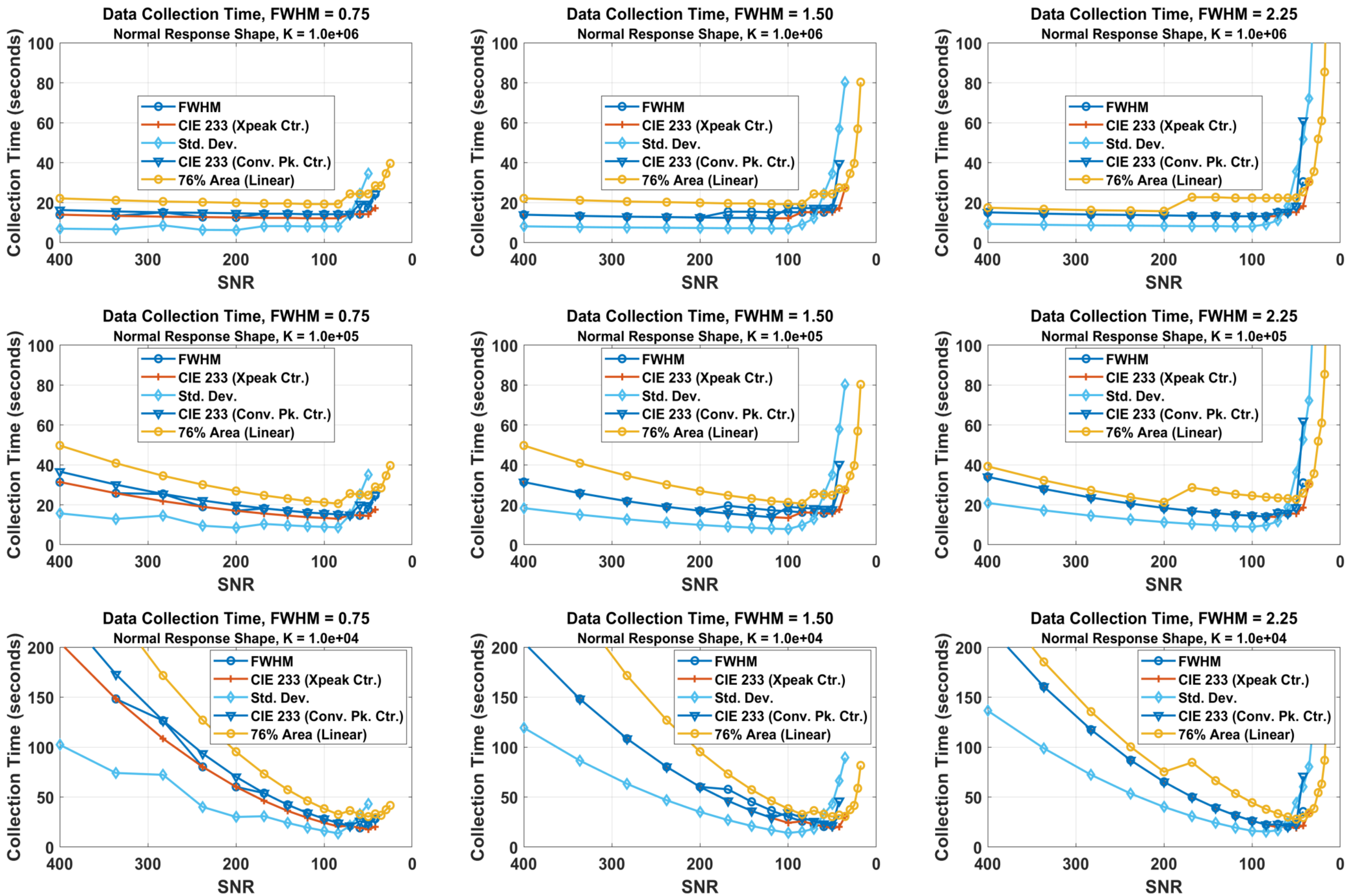

4.3 SNR effects on total test time and algorithm selection (Supplemental information to Fig. 9, width metrics, Bi-Normal responses, all response widths and K-values)